Taking the pulse of nature – How robotics and sensors assist in lake and reservoir management

Sebastian Zug[1*†], Gero Licht[1], Erik Börner[2], Edjair de Souza Mota[4], Roberval Monteiro Bezerra de Lima[3,a], Eric Roeder[2], Jörg Matschullat[2, 5*†]

[1]Institute of Computer Science, Technical University Bergakademie Freiberg, Bernhard-von-Cotta-Straße 2, 09599 Freiberg, Germany

[2]Interdisciplinary Environmental Research Centre, Technical University Bergakademie Freiberg, Brennhausgasse 14, 09599 Freiberg, Germany

[3]Embrapa Florestas, Estrada da Ribeira, km 111, Guaraituba, Colombo-PR, 83411-000, Brazil

[a]formerly at: Embrapa Amazônia Ocidental in Manaus

[4]iComp, Universidade Federal de Amazonas, Av. Gen. Rodrigo Octávio, 6200 Setor Norte do Campus Universitário – Coroado, Manaus-AM, 69080-900, Brazil

[5]Arthur L. Irving Institute, Dartmouth College, 33 Tuck Mall, Hanover, NH 03755, USA

[†]These authors contributed equally to this work and share first authorship

***Correspondence:** Sebastian Zug (robotics and informatics) and Jörg Matschullat (everything else): Sebastian.Zug@informatik.tu-freiberg.de, matschul@tu-freiberg.de (joerg.matschullat@dartmouth.edu)

Keywords: Unmanned surface vehicle, robustness, autonomous field robot, autonomous data aggregation, limnology, Amazon basin

Abstract

Accurate environmental monitoring of aquatic ecosystems is often compromised by field-measurement biases introduced through human presence. Autonomous robotic platforms can mitigate these biases by enabling consistent, long-term data collection under a wide range of environmental conditions. We present the Modular Aquatic Robotic Platform–Freiberg (MARP-FG), an autonomous, catamaran-based system engineered for flexible deployment with customizable sensor payloads to facilitate surface water monitoring.

This paper outlines the design criteria, engineering challenges, and solutions implemented to ensure reliable, autonomous operation. The platform supports modular catamaran floaters sized between 1.2 and 2.5 meters, selected according to payload mass and mission requirements. To demonstrate versatility, three payload configurations were developed and validated: (i) hydrographic profiling via multi-parameter probes, (ii) sonar-based three-dimensional mapping of complex basin morphologies, and (iii) dynamic closed-chamber measurements of greenhouse gas fluxes equipped with onboard CO_2 quantification using infrared spectrometry and automated gas sampling for subsequent gas chromatographic analysis.

Focusing on the greenhouse gas flux measurement configuration, we provide a detailed account of the system's autonomous navigation, operational workflow, and performance metrics. The MARP-FG maintained positioning accuracy within ±2 m under challenging conditions including wave heights up to ±40 cm and wind speeds up to 7 m s^{-1}. Deployments in diverse aquatic environments, such as Amazonian lakes and Central European water bodies, confirmed the platform's robustness and data quality under adverse weather and nocturnal conditions. These innovations substantially improve automated aquatic monitoring capabilities, offering a versatile tool for long-term geoscientific data acquisition.

1 Introduction

Limnologists, biogeochemists, and geoecologists in both academia and water authorities strive to deepen our understanding of how aquatic ecosystems respond to global environmental changes. Their overarching goal is to enhance ecosystem resilience and preserve biodiversity and aquatic ecosystem services. This requires robust methodological solutions. To provide reliable data and secure high-quality water for the public and ecosystems, perpetual, careful, and accurate observations are essential. Surface waterbodies require regular sampling of the water column and hydrographic profiling (acquisition of physicochemical parameters from surface to bottom). This should be done once a month at reservoirs, for example in Germany (ATT 2021), and about once a month for surface waters in the US (Riskin et al. 2018), or quarterly as recommended by the European Water Framework Directive (Ziemińska-Stolarska et al. 2019). Such frequencies are likely suboptimal given the potential risks of intentional or accidental disturbances (spills, contamination, etc.). Marcé et al. (2016) present related challenges and demands of reliable and trustworthy waterbody monitoring. While less frequent, these important tasks include 3D imaging of basins and their sedimentary structures (Fang et al. 2023), high-resolution assessment of greenhouse gas fluxes (CO_2, CH_4, N_2O) between a waterbody and the atmosphere (Huttunen et al. 2003), and other specialized studies, such as the occurrence of micro- and nano plastics in the water column (Strungaru et al. 2019; Triebskorn et al. 2019).

Today's standard monitoring cannot be carried out under adverse weather conditions (e.g. thunderstorms) or at night because of the potential risk to personnel. Robotic monitoring is the solution to minimize associated risks, improve the accuracy and precision of data collection, and increase the frequency of observations (Dunbabin and Marques 2012). This is not new. Many different approaches exist (e.g., Dunbabin and Grinham 2010; Hitz et al. 2014; INTCATCH 2023; Jeong et al. 2020; Melo et al. 2019; Mendoza-Chok et al. 2022; Rajewicz et al. 2022). However, current solutions are often not fit for purpose, since they are heavy, bulky, and costly, resulting in limited flexibility and versatility.

We designed and tested the custom-built catamaran-body-based autonomous Modular Aquatic Robotic Platform-Freiberg (MARP-FG; Fig. 1) based on the development of a versatile and robust closed dynamic chamber system for terrestrial applications (Oertel et al. 2016; Pape et al. 2009; Rochette et al. 1997). Following development and many tests in Germany, we deployed this robotic platform to freshwater lakes in the state of Amazonas, Brazil, to investigate their role in the global carbon cycle (Matschullat et al. 2024). We chose the Amazon basin as our experimental region because we knew that equipment that withstands its harsh climatological conditions (high temperatures with very high radiation and humidity) is robust enough to be used anywhere in the world. Our goal was to develop a platform that could:

a) be transported easily (air and vehicle transport),

b) quickly switch between different payloads (modular design),

c) operate safely even under harsh conditions, including

d) nighttime deployment, which would be too risky for human presence.

The team repeated this investigation in a multi-year campaign (Projects RoBiMo [EU] and RoBiMo-Trop [DBU and IB]), continuously improving the robots along the way. Our main research questions (RQ) for developing our platform and related hypotheses (H) were:

RQ 1 What unique measurement and operational requirements arise when conducting autonomous missions in the inner wet tropics compared to temperate regions of Europe? Which additional technical conditions must the robot design and its sensory array accommodate in these tropical setting?

H1: While the configuration and extent of the measurement campaigns remain the same, tropical weather conditions are the largest source of error when implementing an autonomous measurement system. At the same time, there is no possibility of direct access via a mobile phone network.

RQ 2 How small (and light) can a floating platform be to remain easily transportable and still function reliably under typical conditions of freshwater ecosystems in all climate zones?

H2: A catamaran shape can be small enough to fit mounted onto a standard vehicle, light enough to be accepted in international air traffic, and robust enough to withstand extreme temperatures and humidities.

RQ 3 Which hardware/software architecture provides flexibility while maintaining testability and error tolerance?

H3: A clear separation of tasks – here, data collection and autonomous navigation – ensures both the expandability of the setup and the robustness of the overall system.

RQ 4 How to ensure that error states can be recognized as fast as possible?

H4: To detect and address not intended states or behaviors under harsh conditions, a multimodal approach is required for error identification and communication. This approach should consider the situation's specifics such as limited communication bandwidth, necessary information content, and intervention capabilities.

2 Methods

Earlier developments implemented a platform for mapping water bathymetry using multibeam sonar, as well as a platform for transporting a winch-based system with multi-sensor probe determination of hydrographic profiles (Fig. 1). Its footprint covers approximately 2.5 m x 1.4 m. These systems are too large for convenient transport, however. A redesign of the autonomous platform was therefore required to ensure its ability to work flexibly in the Amazon Basin environment and move quickly between waterbodies. This section outlines the technical implementation and parallel hazard analysis, starting from general requirements and local boundary conditions, to ensure the required robustness.

2.1 Essential requirements and local constraints

The platform must be configured to allow for easy transport by aircraft and in operational state by a standard vehicle. A modular structure must be created enabling simple on-site assembly and quick payload exchange. The robot must be as unobtrusive and quiet as possible for its environmental work and have minimum draft to maneuver over very shallow terrain (≥ 20 cm).

The platform must not travel more than 2.5–3 km from the base station to permit retrieval by boat in case of malfunction, even under unfavorable wind and current conditions. The robot should work an entire workday with a single set of batteries. This will cover total travel distances of up to 10 km and allow for nine gas measurement cycles of 30–45 minutes each. Hot battery swap at the base station is desirable. The team defined the goal for the robot to work under nighttime conditions at the project's outset.

Air temperatures can exceed 40 degrees Celsius in the Amazon Basin. Under direct sunlight, surface temperatures can rise to 60 degrees Celsius; water temperatures reach up to 35 degrees Celsius. Solar radiation (ca. 17 MJ m^2 day^{-1}; Malhi et al. 2022) and air humidity (77 % in the dry season, 88 % in the rainy season; Met Office 2024) are mostly very high. Severe weather with tropical storm precipitation and strong winds is common. Road conditions can be bad, exerting strong mechanical stress on any construction and to electronics during transport. The investigated lakes showed water depth from < 0.5 to > 30 m (Matschullat et al. 2024). The platform must be able to reliably operate under these conditions.

For positioning, ideally Real-Time Kinematic positioning (RTK) should be provided. That solution is possible with two options: i) a physical reference station locally installed or ii) receiving data from an existing one in Brazil via the Internet. Option i): Here, we would have to add a radio link to connect the station and robot. Related to the context – the limited height of both systems' antennas and firm water surface damping effects – this is a challenging task. Option ii): This solution would always require an internet connection, likely unavailable in many scenarios.

In line with our approach to reducing complexity, we chose not to rely on an RTK reference station. Our focus was on developing a robust and self-contained system that performs reliably without depending on external infrastructure. The selected components are widely available and can be sourced in many countries worldwide during a campaign, ensuring operational flexibility and maintainability in diverse environments.

Mobile phone or WLAN connections are limited in the operating area. The robot and devices (base station, monitoring tablets) can reliably exchange actual data and state information in a local network only. Its range is limited without additional antenna technology. The robot will encounter people as some of the measurements take place in cultivated landscapes. The platform must be presented as a research platform with environmental tasks. Furthermore, we must seize every opportunity to explain the robot's concept and functional principle to interested parties. The team was aware that the robot could not be protected in the event of a physical attack (which we never experienced).

To determine gas exchange (specifically CO_2, CH_4, and N_2O) between a water body and the atmosphere, a fast on-board spectrometer is essential for direct CO_2 quantification. Additionally, the ability to sample gases for subsequent gas-chromatographic analysis in a laboratory is necessary. Ambient parameters (water temperature, air temperature, pressure and humidity, photosynthetically active radiation-PAR, and wind speed) must be registered in high temporal resolution parallel to gas analysis and sampling. This is essential to evaluate the obtained gas data. The robot must maintain a stable position within a range of at least ±3 m regardless of wind and wave dynamics when measuring gas exchange (see section 2.4).

2.2 Realized design for platform and payloads

The team developed a custom design in our workshop to meet the handling and campaign requirements, including maximum size and payload, integrated multimodal sensors (Table 1), and platform stability issues. The MARP-FG catamaran platform is based on two fiberglass floats (each approximately 120 x 20 x 20 cm, LxWxH) connected by a universal aluminum frame (4 x 4 cm). It is easily dismountable (Fig. 2). Quick-release fasteners allow for quick exchange between payloads firmly attached to a second aluminum frame.

The total weight is between 20 kg (mounted platform) and up to 50 kg (with sonar), depending on the payload. We focus here on the 'chamber system' configuration for greenhouse gas exchange measurements (ca. 32 kg; Fig. 2, Table 1). The vertical and straight interior sides of the floaters, in combination with deflectors mounted onto the movable chamber, guarantee perfectly still water conditions inside the chamber during measurements, regardless of wind shear, waves, etc. This is a perfect solution for undisturbed gas exchange determinations. The platform, including thrusters, batteries, and a steering unit, cost approximately €3,000. The chamber system with all associated sensors costs an additional €3,500, including the gas sampling unit. The bridge with micrometeorological sensors costs about €1,500, bringing the total for a fully functional system to €7,500 (plus land-based receivers/laptop computers; prices from summer 2024).

The design strikes a balance between manageable size and stable motion and positioning on the water, even under more challenging weather, wind, and current conditions. Two centrally mounted electric thrusters (625 W each; T200, Blue Robotics Inc., USA) propel the boat, allowing top speeds of 5–6 km h^{-1} with the chamber system as payload. These thrusters can be fine-tuned to keep the platform in place with a positional stability of ± 1–2 m^2 (Fig. 6). With thrusters and payload, a draught of 15 cm is achieved, allowing the platform to cruise in shallow water. Four rechargeable batteries (5.2 Ah, 18 V, Einhell, Germany) provide up to 8 hours of system operation. The battery management system supports hot swapping (battery replacement while the application is running), making the system more flexible. A high-resolution (accuracy ± 1 cm) sensor (Ping Sonar Altimeter and Echosounder, Blue Robotics Inc., USA) permanently records the water depth (Table 1) – and warns against running aground.

Box 1 (yellow at the stern in Fig. 2) contains the power supply, a high-resolution GNSS receiver, and an inertial measurement unit (accelerometer, gyroscope, compass) to collect additional navigation information. The gray box at the bow is the actual control unit of the chamber system. It houses a web server for intermediate access to the current state of data aggregation (Fig. 2). In addition to position information and gas concentration, the robot records wind speed and direction, water depth, temperature, humidity, and ambient light (PAR) information, necessary for evaluating gas exchange data. Box 2 (yellow in Fig. 2) contains the 3D-printed xy-driven, 10/20 mL syringe-based gas sampling unit that draws gas from the chamber to feed 18 Exetainer® flasks at discrete times (Fig. 4). The unit enables three gas sampling sequences for subsequent analysis of CO_2 and other gases. The sampling unit is connected directly to the chamber via valve-controlled silicone tubing (not shown in Figs. 2 and 4).

The platform takes off from shore and autonomously navigates to its pre-defined position(s), like aerial drones. Course and experimental sequence are pre-programmed at the base station (https://ardupilot.org/planner/). The human pilot is still responsible for ensuring that the route is navigable and free of obstacles. The robot then automatically executes the planned route and the assigned measurement processes, including autonomous navigation and continuous monitoring of the actual measurement process (Fig. 3). When a task is completed, the platform can move to the next position and restart working. At the end of a site measurement, the platform returns to its starting position (Fig. 3b). In case of error, the mission is aborted, and the robot returns to the base station. Throughout the mission, live data transmission allows monitoring of the measurement and navigation processes (Fig. 3a). A radio link between the robot and the remote control, as well as between the robot and a laptop or smartphone, supports manual intervention.

The hardware/software architecture of the system is divided into two components: i) navigation and ii) the actual measurement unit. Their strict separation simplifies the development process, decouples the systems in case of failure, and ensures fast adaptation to new measurement tasks/sensor setups. Figure 3a illustrates the basic structure and interactions. Autonomous navigation, based on a commercial Pixhawk controller (STM32 controller inside), is implemented (left side), an ESP32 controller realizes measurements and data aggregation (right side). The Pixhawk controller is widely used in aerial drone applications and integrates open software/hardware implementations at different levels of the autonomous navigation process. In our setup, the Pixhawk runs a customized version of the Ardupilot software stack. The ESP32 implements the actual CO_2 measurements and records environmental parameters (such as water temperature and depth, PAR and micrometeorology). This part can be changed to another setup for alternative missions (modular design). The communication interfaces of both microcontrollers can be addressed wirelessly by the pilot. The Pixhawk provides a standardized telemetry interface to interact with the base station using the 'MAVLink' standard, which works up to about 500 meters over water. A web server is also run on the ESP to display live measurement status on a cell phone or laptop browser. This means that the supervisor has access to all parameters (autonomous navigation, current data from the gas bell) and can intervene, if necessary, at least over short distances.

2.3 Application in a pilot study in humid tropical freshwater environments

Five lakes in the state of Amazonas, Brazil, were selected for five field campaigns, covering two wet seasons and three dry seasons from September 2021 to August 2023 (Matschullat et al. 2024). Artificial Balbina reservoir, located about 180 km north of Manaus, the capital of Amazonas State, Brazil, is a clearwater lake, filled in 1984. Blackwater lakes of the Negro River water type were represented by the Caldeirão and Jandira lakes on the Iranduba Peninsula (between the Negro and Solimões Rivers). Lakes Iranduba and Grande represented whitewater lakes of the Solimões (Amazonas) River water type. The project website shows the locations of the lakes on a map (https://sebastianzug.github.io/RoBiMo_Trop_DataSet/; Zug 2023; see also supplement figure S1).

2.4 CO_2 exchange, analytical methods and boundary conditions

To determine CO_2 exchange, a closed dynamic chamber system was mounted to the upper quick-release aluminum frame. The custom-built chamber automatically tilts up above the water for flushing between measurements and for safe travel and transport (Fig. 2). To record a measurement, the chamber tilts down. Its base then sits 3–4 centimeters below the water surface to prevent atmospheric air from being drawn in. An infrared spectrometer (GMP-252, Vaisala, Finland) takes high-resolution CO_2 measurements at 1-second intervals. The two deflector shields mounted on the chamber between the two floats drastically reduce wave motion and currents around the chamber (Fig. 2). A fan inside the chamber provides gas homogenization during the accumulation period.

At each position, the measurement sequence consists of three repetitions (approximately 6 minutes each) of CO_2 determinations with intermittent purging. A fourth repetition starts an automatic parallel gas sampling series. Each series consisted of six samples taken at equal time intervals (approximately 30 minutes total) and stored in double septum 12 mL Exetainer® flasks (Labco, England). At the end of a series, the chamber tilts up for flushing; the platform can move to the next predefined position. All sensor parameters are permanently logged. After gas drying steps in the laboratory, the samples from the Exetainers were analyzed for CO_2 plus methane (CH_4) and nitrous oxide (N_2O) by gas chromatography (SRI Instruments 8610C, USA) in Freiberg under thorough quality control.

3 Mechanisms to increase robustness

Field research with technical equipment often faces difficulties when parts of the system fail. Limited repair capabilities in the field and a potential lack of communication options in remote regions can significantly hamper or even fail a measurement campaign. Unpredictable failures can be categorized according to the different phases of a mission (Table 2, columns 1 and 2). Based on this categorization, the team performed a hazard analysis during the MARP-FG design process to identify potential sources of failure, considering the system architecture, operating conditions, and technical components. This failure list was continuously updated with the experience of each campaign. The third column in Table 2 provides examples of individual error sources. Each error was mapped to three types of strategies (St):

St1. Incorporating improvements into the design to eliminate faults,

St2. Developing an operational avoidance strategy to minimize the likelihood of error occurrence, and

St3. Including the error in the project's monitoring concept, making the error status explicit and visible to the observer.

The continuous improvement of the technical design led to protective covers for prominent sensors (Table 2: 1a), extensive routing of cables in appropriate channels, and the introduction of two pendulum flaps to stabilize the water between the catamaran floats (Table 2: 6d). An example of the avoidance strategy is the procedure for aggregating and handling the data collected by the robot (Table 2: 7cd). After each mission, the team needed to minimize the chances of data loss. A detailed procedure model was designed to describe the processes for removing the SD card from the navigation unit and reading the data from the gas bell. Accordingly, the procedures first required the shutdown of the entire system, a prohibition on removing the storage media near water, and an immediate multiple copy operation for at least two independent storage devices. At least one of these copies had to be checked for file consistency. Data loss was therefore ruled out at this stage of the project.

However, it was not possible to find a suitable avoidance strategy for all potential errors. In particular, the complex software structure with the two sub-areas of autonomous navigation and control of the measurement system and their interaction opened the possibility of software errors (Table 2: 4ab). The aim was to ensure early detection so the error could be rectified immediately in the field by repairing or restarting the system. The variety of errors, the need to display the error

status over different distances, and the challenges of the application made it clear that a standardized interface for error communication was not appropriate. As a result, several channels, some of them redundant, were set up (Table 3 in descending order of distance).

The composition of the different error communication channels reflects the specific requirements of the RoBiMo-Trop campaign. The robot should operate on water during day and night. For safety reasons, the robot should not be accompanied by the normally used dinghy in the dark. Therefore, communication of the robot's states had to be provided up to a maximum distance of 2.5 km, without 3G to 5G cellular connection. Direct radio communication with the telemetry unit is not robustly possible over open water at ranges greater than 500 m. Following these constraints, three patterns of online mission monitoring were implemented in the field tests that can be considered successful:

1) During the first daytime missions, team members followed the robot closely in a small boat. Continuous visual and data-driven monitoring ensured that errors were detected quickly (Table 2 Error Classes 1, 2, and 3).
2) During the night missions, the first measurements were made only in the immediate vicinity. In the telemetry area, the correct behavior of the robot was tested with a few measurement points. After that, the MARP-FG operated autonomously at the maximum distance.
3) Due to the limited bandwidth and range of wireless communication, a complete online evaluation of the entire data set is impossible. Therefore, it was necessary to check the results offline after each mission. Table 3 highlights these methods in gray.

The following paragraphs describe the implementation of the four channels mentioned in Table 3 as strategies for error communication: Position lights and LED beams, webserver for state representation, automated gas sampling unit and the data processing chain.

Position Lights and LED Beams. The position lights and LED lighting enable the robot to be localized during night missions and to visualize its status. Since the initial LED strip was not bright enough to display the position over 2500 meters, the team integrated position lights. These simple solar-powered LED lamps were mounted on the bridge next to the antennas on the left and right. Their luminosity was so strong that the illumination was also very useful for preparing the platform and for manual navigation, considering the vegetation along the shore as well as floating plants.

The LED strip with a WS2812B chipset could not perform the intended task. It was supposed to visualize different phases of the mission implementation (Figure 2b) and communicate navigation-specific errors such as low battery level, increased current consumption of the motors, and missing GNSS position information. Due to time constraints, the state-dependent color selection from the PixHawk has not yet been implemented. The team integrated an additional microcontroller responsible for initializing and controlling the LEDs. However, these LEDs then displayed a static pattern that indicated the direction of the robot based on the colors (conventional navigation lights).

Webserver. The web server (Figure 5) provides direct access to the parameters of the gas chamber measurement process and currently recorded values. This includes supplementary sensors for measuring environmental conditions. The functionality was implemented as a task within the FreeRTOS-based software structure of the ESP32. For performance reasons, it was assumed that only one client would be connected at a time. Due to the assumed lack of internet connectivity in the operational area, all necessary JavaScript libraries used for graphical representation were stored locally on the ESP. This allowed the client’s browser to retrieve them directly from the main webpage. Using a tablet or mobile phone for this interface proved effective. However, despite an external antenna for the ESP, the communication range was very limited. Stable communication was only possible up to 20 meters.

Gas sampler. Parallel to the continuous measurement of the gas composition in the chamber during measurements, the MARP-FG activates a sampler that transfers gas from the chamber headspace into Exetainers®. The redundant data collection enables us to check the plausibility of the digitally recorded CO_2 values afterwards and to evaluate additional gases (here CH_4 and N_2O).

The gas sampler itself consists of a pump system with a capacity of 10 mL per stroke (Fig. 4). Before the actual sampling, the system first flushes all lines with air from the chamber. The sampler then moves the needle to the position of the next free Exetainer® and inserts it into the vacuumed glass tube, which is sealed with a rubber membrane (double septum). The setup comprises a total of 6x3 pre-labeled Exetainers®. The sampler integrates several error identification methods that are designed to detect if, for example, the needle has become stuck, the needle positioning does not reference an Exetainer® flask or that a flask was not filled completely.

Figure S2 illustrates general observations comparing in-situ (on lake) CO_2-measurements with subsequent laboratory CO_2-determinations based on the gas samples collected concurrently with the on-board quantification using the Vaisala sensor. The on-board Vaisala sensor tends to deliver systematically lower mixing ratios as compared to the gas-chromatographic determination of the gas sampled obtained in parallel. This does not affect the flux calculation however, since the curves show similar behavior. We generally use the results from both methods in analyzing and interpreting the data.

Log file analysis. The measurement and the robot control system store the collected data on individual memory cards. The Pixhawk records all robot-specific information (steering commands, control states, navigation parameters, internal robot states, battery system data) in standardized Ardupilot mission files; the ESP32 logs the measurement data in CSV format (Fig. 3). The Ardupilot log files contain all configuration parameters of the navigation unit and tracks of measurements/robot states with individual sampling rates (https://ardupilot.org/copter/docs/logmessages.html). These logging parameters are highly parameterizable (https://ardupilot.org/copter/docs/common-downloading-and-analyzing-data-logs-in-mission-planner.html#common-downloading-and-analyzing-data-logs-in-mission-planner). Given individual problems with radio outages due to long ranges and limited bandwidth, we did not consider the telemetry data set for remote transfer, the second log chain available for Ardupilot. Accordingly, these logs do not cover the entire mission records.

All aggregated information is processed offline in a Python-based toolchain (https://sebastianzug.github.io/RoBiMo_Trop_DataSet/; Zug 2023). The implementation merges robot state information from the Ardupilot log files and the measurement data in five steps:

1. The raw data aggregator evaluates and homogenizes the individual files. It maps the content on Pandas' data frames (Pandas: RRID:SCR_018214). The binary log files were transferred on text files in a first step and searched for specific log samples (estimated position, AHR2, GNSS position measurements, GPS, and sonar outputs, RFND_Dist) by a python script at a second stage. For this purpose, an existing open source implementation was adapted for a selective access on sets of large log files (https://gitlab.rrz.uni-hamburg.de/bay2789/bslogfiles/-/tree/master).
2. At a second stage the pipeline merges the position and measurement data using the time stamps. The necessary synchronization took place on the Pixhawk via the GNSS measurements while the ESP obtained a time stamp once at the beginning of the measurement via the connection with a mobile device (laptop or smartphone).
3. For a decomposition of the tracks a cluster analysis was implemented to investigate the movement behavior of the robot in the vicinity of the manually selected measurement positions. Based on the dwell time at these points, the spatial position was extracted using a k-means approach. The number of clusters varied per water body. At the same stage, corresponding statistical key figures (min, max, std) of the water parameters (CO_2, temperature, depth, etc.) are summarized.
4. The visualization includes the georeferenced representation of the robot movements for the individual measuring points (Figures 3, 6). The script generated both an overall overview and a measurement point-related representation of the autonomous robot's movements. For the analysis of the robot behavior, position fidelity was important. Figure 6 shows the distributions and indicates maximum horizontal (2.6 m) and vertical (4.0 m) deviations. However, the

histogram clearly shows that most of the measuring points were much closer to the intended position. Based on the analyses, adjustments could be made to the control parameters.

5. Step 5 automatically generates the web pages containing graphics and data. This concerns both the representation of the robot's movements (exemplary https://sebastianzug.github.io/RoBiMo_Trop_DataSet/html/balbina.html) and the tabular processing of the measurement results for immediate evaluation and the planning of further missions on a body of water (https://sebastianzug.github.io/RoBiMo_Trop_DataSet/html/interactive_table.html).

The software was realized as a collection of Jupyter notebooks, executed as a pipeline based on the papermill python package (https://github.com/nteract/papermill) when a new data set is available as a public GitHub project (Jupyter Notebook: RRID:SCR_018315; GitHub: RRID:SCR_002630). With this implementation, the data from MARP-FG can be analyzed daily in parallel with the measurement campaign and visualized on a website. This enabled the team to constantly review their measurement strategy and adapt the setup.

4 Results and discussion

While most of this work relates to the methodological platform development and its payload optimization, the next two sections present key results of these efforts and discuss them in relation to our initial research questions and hypotheses.

4.1 Robotics and Informatics

Starting with a first prototype in 2020, an all-manual catamaran and an early version of the chamber system, our robotic platform is currently in its 4th development stage (Fig. 7). Each stage added sensors and capabilities. The platform became increasingly more flexible and autonomous, leading to its current state of full autonomy. Larger antennas proved very useful in extending the range of the vehicle when direct communication during a run was required (Delock 88450 WLAN; 352.1 mm long). Two information pipelines (Figure 3) were developed to evaluate errors, inaccuracies, and malfunctions.

The entire construction, including the gas exchange payload (mounted on the second, upper aluminum frame), works well up to wave heights of about ±40 cm and wind speeds up to about 7 m s^{-1}. Beyond these values, the platform can still maneuver but does not perform reliable gas exchange measurements, 3D mapping or hydrographic profiling.

The catamaran-type platform body presents maximum stability under most weather conditions and allows for comparatively heavy payloads. Average inner moist tropical boundary conditions can easily be dealt with. All components resisted significant rain and windstorms; we did not face data losses. In more remote environments with minimum nighttime luminosity, the additional mount of position lights on the bridge is highly recommended. We successfully used Velcro-strap attached Solar battery-powered LEDs.

The mid-board thruster positioning proved to be better than conventional stern positioning, since it allows for minimum turning space and operation in demanding environments, such as water surfaces with thick carpets of macroalga or other plant and drift materials. Figure 5 shows an example of a real mission at Lake Caldeirão, Amazonas, Brazil: Position 2 was targeted four times by MARP-FG. The maximum difference in horizontal (x) and vertical (y) directions was 2.6 and 4.0 m, respectively. The two histograms attached to the trajectories in x and y direction show that these maxima were outliers.

The multimodal error communication concept has proven its worth. All error states were quickly identified regardless of whether

- material got caught in the propellers,

- the state machine of the measuring process blocked due to communication interruptions during command transmission, or
- the gas sampler blocked due to a shifted Exetainer® position.

The only points of criticism during the last campaign refer to missing state information, represented by the LED bar, and the clarity of the position lights. The first aspect would have eliminated the need for manual checks of the web server and telemetry data upon detecting an error. Local error interpretation and visualization would have further enhanced convenience. The latter did not allow for a clear indication of the robot's current direction of movement over long distances, especially during the night missions, even with good visibility.

4.2 Biogeochemistry – Geoecology – Limnology

These scientific fields contribute to Earth System Science and are particularly interested in freshwater ecosystems and their role in the global carbon cycle (e.g., Friedlingstein et al. 2023; Raymond et al. 2013). Our entire platform development (MARP-FG) was initially motivated by the need to produce high quality data at all times of day and under sometimes harsh meteorological conditions in the Amazon Basin, Brazil, with limited available funding. The step-by-step development of hardware and software proved helpful in reducing the complexity of errors and malfunctions – and enabled successful field campaigns right from the start.

The MARP-FG allows work under the forest canopy during the wet season when water levels are high, and lakes occupy a much larger surface area than during their low water conditions in the dry season. The slim, low-profile design can maneuver through thickets that are impassable to people in a small boat. The almost inaudible hum of the thrusters, the chamber mechanism and the internal fan noise do not deter animals. While large mammals such as Amazon river dolphins (*Inia geoffrensis*) have curiously explored the platform, they have never attacked or interfered with measurements and sampling. Even at night, the platform is inaudible for humans at about 10 m from the operators.

Determination of greenhouse gas fluxes requires daytime and nighttime data collection (Oertel et al. 2016; Pape et al. 2009; Rochette et al. 1997). Related work on water bodies is still scarce; no homogenized methodology exists. Solutions range from very simple makeshift floats carrying an equally simple chamber (neither of which is robust or able to operate autonomously or at night), to larger manned platforms with more sophisticated chamber systems or eddy covariance towers (Podgrajsek et al. 2014) that are expensive and cumbersome to transport.

Starting with a closed dynamic chamber system developed for soil gas exchange assessment (Oertel et al. 2016), we realized that this model was too large and heavy, and that the Vaisala GMP 343 sensor was suboptimal with its higher energy demand. In addition, the transparent chamber design was not necessary. With the resulting smaller dimensions and lighter construction, our redesigned chamber system could better cope with the aquatic environment. The straight vertical board between the floaters was a necessity for the payload "chamber system" and associated gas sampling to achieve truly calm water conditions during measurements.

When using the chamber system to measure CO_2 gas exchange in the field and to sample greenhouse gases, the CO_2 data may vary (within acceptable limits) between the on-board determination by IRGA and the samples taken by the automatic sampler, and subsequently analyzed by gas chromatography (Figure S2). Such a difference depends on 'humidity', 'wind speed' and 'wave action' and can be explained by the sensitivity of the Vaisala sensor to water spray and ambient humidity in general, while the automatically collected gas samples are dried prior to gas chromatographic species identification, homogenizing them for subsequent analysis.

Obtained CO_2 determinations remained constant and highly reproducible throughout. Distinct day/night differences in gas exchange could be confirmed as reported in the literature (Sieczko et al. 2020). Our new data do not show significantly higher emissions from the water bodies compared to the surrounding soils under forest canopy or agricultural land use (Matschullat et al. 2021). Lake

boundary conditions are available (Matschullat et al. 2025). A corresponding manuscript on the gas fluxes is in preparation, data will be uploaded to the Pangaea data publisher (https://www.pangaea.de/); interested readers are welcome to contact the authors for more details.

5 Conclusions

Robotic water monitoring and sampling can reduce bias and increase data accuracy and precision due to improved positional accuracy and track repeatability, as well as the absence of human disturbance (movement, noise, odor). Reduced risk to personnel and the ability to operate under more challenging conditions, such as night and bad weather, are additional benefits. The MARP-FG platform stays in position during measurements and sampling with an average accuracy of 1–2 meters (X-Y-directions) and revisits pre-defined positions with the same precision. The relatively low mass of the platform drastically reduces any unwanted "pumping" effect of a water column on gas exchange measurements compared to manned boats, and the platform dimensions allow it to navigate in shallow water as well as under overhanging tree or brush canopies.

Measurements of water column and surface parameters were spatially reproducible and provided high-resolution data, important for assessing water quality in lakes with varying bottom morphometry, spatially confined (underwater) inflow areas, and for specific experimental designs requiring observation of spatial phenomena in high temporal resolution.

Our initial platform development questions were answered as follows:

RQ 1 The floating autonomous robotic platform MARP-FG is easily transportable (standard vehicle, air transport) and operates reliably in typical freshwater environments in all climate zones, including harsh weather conditions. During the five campaigns in the Amazon Basin, as well as numerous campaigns in Central Europe, the platform operated reliably in all weather conditions, including strong storms and wave heights above ± 40 cm, as well as at night. With charged backup batteries, 24-hour campaigns are possible (hot swapping).

RQ 2 Depending on the payload, the MARP-FG weighs between 20 and 100 kg. Equipped with the "chamber," the robot weighs 32 kg and has external dimensions of 120 x 70 x 80 cm (LxWxH). The catamaran-type floater design proved to be ideal for the defined tasks. Components with maximum reliability even under harsh environmental conditions (e.g. sensors, thrusters, etc.) exist and are freely available on the market,

RQ 3 A separation of robot control and data acquisition on two layers decouples the components and supports individual error detection and reaction mechanisms. Hence, this configuration ensures a robust behavior of the MARP-FG platform during long term missions.

RQ 4 Effective robotic field operation requires more than simply integrating multiple communication methods; these methods must be integrated within a comprehensive error detection framework that reliably identifies—and where possible prevents—platform uncertainties. This paper presents our methodological approach to achieving this goal.

For gas exchange measurements and hydrographic profiling in particular, robotic platforms minimize errors associated with the disturbance caused by the larger mass and physical presence of manned boats, such as the pumping effect on the water column. Given the substantial diurnal variability of environmental parameters, our robotic system enables both nighttime and daytime measurement series, allowing for more comprehensive temporal coverage. Our initial key research questions have been addressed to a satisfactory extent; however, further validation in subsequent field campaigns remains necessary.

Conflict of Interest

The authors declare that the research was conducted in the absence of any commercial or financial relationships that could be construed as a potential conflict of interest.

Author Contributions

SZ: Conceptualization, Data curation, Investigation, Methodology, Resources, Software, Supervision, Validation, Writing; GL: Data curation, Methodology, Software, Validation; EB: Conceptualization, Methodology, Resources, Software; RMBL: Funding acquisition, Project administration, Resources, Supervision; ER: Investigation, Validation; EM: Resources; JM: Conceptualization, Data curation, Formal analysis, Funding acquisition, Investigation, Methodology, Project administration, Resources, Supervision, Writing.

Funding

The EU-funded (ESF) project 'RoBiMo' laid the foundation for the development presented here, which was funded by the German Federal Ministry of Education and Research (BMBF; FKZ 01DN21018) through its International Bureau (IB), and the Deutsche Bundesstiftung Umwelt (DBU; Az 36095/01).

Acknowledgments

This work is part of the RoBiMo-Trop project (Robotic Monitoring of Freshwaters in the Tropics), generously supported by the German Federal Ministry of Education and Research and the Deutsche Bundesstiftung Umwelt. We sincerely thank these organizations for their essential support, without which this project would not have been possible. We also acknowledge the European Science Foundation (ESF) for their support of the preceding RoBiMo project, which provided the foundational hardware and software developments for our work.

We extend our gratitude to Embrapa Amazônia Ocidental in Manaus for generously providing technical infrastructure. We are especially thankful to Gilvan Coimbra Martins (Embrapa) and Séan P.A. Adam (TUBAF) for their invaluable assistance and support during fieldwork.

References

ATT (2021) Untersuchungsprogramm zur Wasserbeschaffenheit in Trinkwassertalsperren. (*Study program in water quality in drinking water reservoirs*) Arbeitsgemeinschaft Trinkwassertalsperren e.V. (ATT) Technische Information 8: 25 p (ISBN 3-486-26472-9) – in German.

Dunbabin M, Grinham A (2010) Experimental evaluation of an autonomous surface vehicle for water quality and greenhouse gas emission monitoring. 2010 IEEE International Conference on Robotics and Automation: 5268–5274; doi 10.1109/ROBOT.2010.5509187.

Dunbabin M, Marques L (2012) Robotics for environmental monitoring. IEEE Robotics & Automation Magazine 20-23; doi 10.1109/MRA.2012.2186482.

Fang C, Lu S, Li M, Wang Y, Li X, Tang H, Ikhumhen HO (2023) Lake water storage estimation method based on similar characteristics of above-water and underwater topography. J Hydrol 618: 129146; doi 10.1016/j.jhydrol.2023.129146.

Friedlingstein P, O'Sullivan M, Jones MW, Andrew RM, Bakker DCE, Hauck J, Landschützer P, Le Quéré C, Luijkx IT, Peters GP, Peters W, Pongratz J, Schwingshackl C, Sitch S, Canadell JG, Ciais P, Jackson RB, Alin SR, Anthoni P, Barbero L, Bates NR, Becker M, Bellouin N, Decharme B, Bopp L, Brasika IBM, Cadule P, Chamberlain MA, Chandra N, Chau TTT, Chevallier F, Chini LP, Cronin M, Dou X, Enyo K, Evans W, Falk S, Feely RA, Feng L, Ford DJ, Gasser T, Ghattas J, Gkritzalis T, Grassi G, Gregor L, Gruber N, Gürses Ö, Harris I, Hefner M, Heinke J, Houghton RA, Hurtt GC, Iida Y, Ilyina T, Jacobson AR, Jain A, Jarníková T, Jersild A, Jiang F, Jin Z, Joos F, Kato E, Keeling RF, Kennedy D, Klein Goldewijk K, Knauer J, Korsbakken JI, Körtzinger A, Lan X, Lefèvre N, Li H, Liu J, Liu Z, Ma L, Marland G, Mayot N, McGuire PC, McKinley GA, Meyer G, Morgan EJ, Munro DR, Nakaoka SI, Niwa Y, O'Brien KM, Olsen A, Omar AM, Ono T, Paulsen M, Pierrot D, Pocock K, Poulter B, Powis CM, Rehder G, Resplandy L, Robertson E, Rödenbeck C, Rosan TM, Schwinger J, Séférian R, Smallman TL, Smith SM, Sospedra-Alfonso R, Sun Q, Sutton AJ, Sweeney C, Takao S, Tans PP, Tian H, Tilbrook B, Tsujino H, Tubiello F, van der Werf GR, van Ooijen E, Wanninkhof R, Watanabe M, Wimart-Rousseau C, Yang D, Yang X, Yuan W, Yue X, Zaehle S, Zeng J, and Zheng B (2023) Global Carbon Budget 2023. Earth Sys Sci Data 15: 5301–5369; doi 10.5194/essd-15-5301-2023.

574 Hitz G, Gotovos A, Pomerleau F, Garneau MÈ, Pradalier C, Krause A, and Siegwart R (2014) Fully autonomous
575 focused exploration for robotic environmental monitoring. IEEE International Conference on Robotics and
576 Automation (ICRA): 2658 – 2664; doi 10.3929/ethz-a-010170418.
577 Huttunen JT, Alm J, Liikanen A, Juutinen S, Larmola T, Hammar T, Silvola J, and Martikainen PJ (2003) Fluxes
578 of methane, carbon dioxide and nitrous oxide in boreal lakes and potential anthropogenic effects on the
579 aquatic greenhouse gas emissions. Chemosphere 52: 609-621; doi 0.1016/S0045-6535(03)00243-1.
580 INTCATCH (2023) http://intcatch.eu/index.php/about-intcatch/intcatch; last access: July 15, 2024.
581 Jeong M, Roznere M, Lensgraf S, Sniffen A, Balkcom D, and Quattrini Li A (2020) Catabot: Autonomous surface
582 vehicle with an optimized design for environmental monitoring. Global Oceans 2020: Singapore – U.S. Gulf
583 Coast, Biloxi, MS, USA, pp. 1-9; doi: 10.1109/IEEECONF38699.2020.9389391.
584 Malhi Y, Pegoraro E, Nobre AD, Pereira MGP, Grace J, Culf AD, and Clement R (2002) Energy and water
585 dynamics of a central Amazonian rain forest. JGR Atmospheres 107, D20: LBA 45-1-LBA 45-17; doi
586 10.1029/2001JD000623.
587 Marcé R, George G, Buscarinu P, Deidda M, Dunalska J, de Eyto E, Flaim G, Grossart HP, Istvanovics V,
588 Lenhardt M, Moreno-Ostos E, Obrador B, Ostrovsky I, Pierson DC, Potužák J, Poikane S, Rinke K,
589 Rodríguez-Mozaz S, Staehr PA, Šumberová K, Waajen G, Weyhenmeyer GA, Weathers KC, Zion M, Ibelings
590 BW, and Jennings E (2016) Automatic high frequency monitoring for improved lake and reservoir
591 management. Environ Sci Technol 50, 20: 10780–10794; doi 10.1021/acs.est.6b01604.
592 Matschullat J, Bezerra de Lima RM, von Fromm SF, Coimbra Martins G, Schneider M, Mathis A, Malheiros
593 Ramos A, Plessow A, and Kibler K (2021) Sustainable land-use alternatives in tropical rainforests? Evidence
594 from natural and social sciences. Eur Geol 52: 5-20; doi 10.5281/zenodo.5769730
595 Matschullat J, Roeder E, and Adam SMP (2025a) RoBiMo-Trop – water chemical, hydrographical profile and
596 sediment chemical data from shallow tropical lakes and one reservoir plus two pisciculture sites in Amazonas,
597 Brazil. Pangaea PDI https://issues.pangaea.de/browse/PDI-38801
598 Matschullat J, Bezerra de Lima RM, Coimbra Martins G, de Lima Boijink C, Dairiki JK, Roeder E, Lau MP, Souza
599 de Oliveira CT, Malheiros Ramos A, Plessow A, Schwatke C, and Forsberg BR (2025b) Water and sediment
600 chemistry of shallow tropical lakes show alert signals. Copernicus Biogeosci (in preparation).
601 Melo M, Mota F, Albuquerque V, and Alexandria A (2019) Development of a robotic airboat for online water
602 quality monitoring in lakes. Robotics 8, 1: 19; doi 10.3390/robotics8010019.
603 Mendoza-Chok J, Luque JCC, Salas-Cueva NF, Yanyachi D, and Yanyachi PR (2022) Hybrid control
604 architecture of an unmanned surface vehicle used for water quality monitoring. IEEE Access 10: 112789–
605 112798; doi 10.1109/ACCESS.2022.3216563.
606 Met Office (2024) Air humidity Manaus, Brazil. https://www.metoffice.gov.uk/weather/travel/holiday-
607 weather/americas/brazil/manaus. Last access: July 15, 2024.
608 Oertel C, Matschullat J, Zimmermann F, Zurba K, and Erasmi S (2016) Greenhouse gas emissions from soils –
609 a review. Chem Erde – Geochem 76, 3: 327–352; doi 10.1016/j.chemer.2016.04.002.
610 Pape L, Ammann C, Nyfeler-Brunner A, Spirig C, Hens K and Meixner FX (2009) An automated dynamic
611 chamber system for surface exchange measurement of non-reactive and reactive trace gases of grassland
612 ecosystems. Biogeosci 6, 3: 405–429; doi 10.5194/bg-6-405-2009.
613 Podgrajsek E, Sahlée E, Bastviken D, Holst J, Lindroth A, Tranvik L, and Rutgersson A (2014) Comparison of
614 floating chamber and eddy covariance measurements of lake greenhouse gas fluxes. Biogeosci 11: 4225–
615 4233; doi:10.5194/bg-11-4225-2014.
616 Rajewicz W, Schmickl T, and Thenius R (2022) The use of robots in aquatic biomonitoring with special focus on
617 biohybrid entities. In Müller A, and Brandstötter M (eds) Advances in service and industrial robotics. RAAD
618 Mechanisms and Machine Science 120. Springer; doi 10.1007/978-3-031-04870-8_61doi
619 10.1038/nature12760.
620 Raymond P, Hartmann J, Lauerwald R, Sobek S, McDonald C, Hoover M, Butman D, Striegl R, Mayorga E,
621 Humborg C, Kortelainen P, Dürr H, Meybeck M, Ciais P, and Guth P (2013) Global carbon dioxide emissions
622 from inland waters. Nature 503: 355–359; doi 10.1038/nature12760.
623 Riskin ML, Reutter DC, Martin JD, and Mueller DK (2018) Quality-control design for surface-water sampling in
624 the National Water-Quality Network: U.S. Geological Survey Open-File Report 2018–1018: 15: doi
625 10.3133/ofr20181018.

626 Rochette P, Ellert B, Gregorich EG, Desjardins RL, Pattey E, Lessard R, and Johnson BG (1997) Description of
627 a dynamic closed chamber for measuring soil respiration and its comparison with other techniques. Can J
628 Soil Sci 77: 195–203; doi 10.4141/S96-110.
629 Sieczko AK, Duc NT, Schenk J, Pajala G, Rudberg D, Sawakuchi HO, and Bastviken D (2020) Diel variability of
630 methane emissions from lakes. PNAS 117(35): 21488–21494; doi: 10.1073/pnas.2006024117.
631 Strungaru SA, Jijie R, Nicoara M, Plavan G, and Faggio C (2019) Micro- (nano) plastics in freshwater
632 ecosystems: Abundance, toxicological impact and quantification methodology. TrAC Tracks Anal Chem 110:
633 116-128; doi 10.1016/j.trac.2018.10.025.
634 Triebskorn R, Braunbeck T, Grummt T, Hanslik L, Huppertsberg S, Jekel M, Knepper TP, Krais S, Müller YK,
635 Pittroff M, Ruhl AS, Schmieg H, Schür C, Strobel C, Wagner M, Zumbülte N, and Köhler HR (2019)
636 Relevance of nano- and microplastics for freshwater ecosystems: a critical review. TrAC Tracks Anal Chem
637 110: 375-392; doi 10.1016/j.trac.2018.11.023.
638 Ziemińska-Stolarska A, Imbierowicz M, Jaskulski M, Szmidt A, and Zbiciński I. Continuous and periodic
639 monitoring system of surface water quality of an impounding reservoir: Sulejow Reservoir, Poland. Int J
640 Environ Res Public Health, 2019, 16(3): 301; doi 10.3390/ijerph16030301.
641 Zug S (2023) Data storage and processing RoBiMo-Trop".
642 https://github.com/SebastianZug/RoBiMo_Trop_DataSet; last access: July 09, 2024.

643 **Data Availability Statement**

644 The datasets for this study can be found in the GitHub repository: [Zug S. Data storage and processing
645 RoBiMo-Trop". https://github.com/SebastianZug/RoBiMo_Trop_DataSet; 2023]; Last access: May 05, 2024.
646

Tables and figures

Table 1. MARP-FG payload sensor types and their specifics as well as producer information (all web pages last verified on May 13, 2025)

Sensor	Measuring range (accuracy)	Links
CO_2-infrared spectrometer GMP-252	0–2000 ppm_v (±18 ppm_v). The sensor can be set to higher concentrations with lower resolution	https://www.vaisala.com/en/products/instruments-sensors-and-other-measurement-devices/instruments-industrial-measurements/gmp252
Combined air humidity-temperature probe DKRF500 EA	0–100 % RH (±1.8% RH) -40 – +80 °C (±0.3°C)	https://www.driesen-kern.com/products/humidity-and-material-moisture/transmitters-and-probes/humidity-temperature-standard-model-dkrf500.php
Temperature probe DKT200	-40 – +80 °C (±0.3°C)	https://www.driesen-kern.com/products/temperature-measurement/temperature-probes/dkt200-temperature-probe.php
Air pressure sensor AMS 4711-1200-B	700–1200 mbar (0.3 % FSO)	https://www.amsys-sensor.com/products/pressure-sensor/ams4711-analog-pressure-transmitter-5v-output/
PAR sensor Apogee SQ 421	1–4000 µmol m^{-2} s^{-1} (± 5 %)	https://www.apogeeinstruments.com/sq-421x-ss-sdi-12-digital-output-quantum-sensor/
Anemometer ATMOS 22	0–30 m/s (±0.3 m/s) 0–359 ° (±1 °)	https://www.metergroup.com/en/meter-environment/products/atmos-22-ultrasonic-anemometer
Precip sensor RG-15	(±10 %)	https://www.antratek.de/optical-rain-gauge-rg-15
Air temp, rH, pressure sensor BME280	-40 – +85 °C (±1.0 °C); 0–100 % RH (±3%); 300–1100 hPa (±1 hPa)	https://www.bosch-sensortec.com/products/environmental-sensors/humidity-sensors-bme280/
Altimeter and echosounder Ping Sonar	0.5–70 m (1–25 cm)	https://bluerobotics.com/store/sensors-sonars-cameras/sonar/ping-sonar-r2-rp/

652 **Table 2**. Potential error sources in different phases of work (A) with field robots. At a general level (B) and a
653 specific level for the described floating robot system MARP-FG (C)

Phase (A)	**Generic, project-/system overarching error sources (B)**	**Error sources in the RoBiMo-Trop project (C)**
Mission preparation	(1) Carelessness when transporting the robot in the field	(1a) Damage to a permanently installed (weather) sensor, (1b) cabling on the robot, (1c) waterproof covers on the robot, (1d) the floats
	(2) Errors during mechanical/electrical system assembly in preparation for a mission	(2a) Incorrect thruster height settings before each use, (2b) Asymmetrical thruster mounting, (2c) Insertion of empty batteries, (2d) Failure to remove protective caps from sensors
	(3) Operating error during software-based mission preparation	(3a) Incorrect specification of the trajectory, (3b) Incorrect adjustment of the thruster control parameters
Mission execution	(4) Software error in the navigation unit or the measuring system	(4a) Crashes of individual components, (4b) Irregular timing of individual tasks
	(5) Hardware errors	(5a) Random disturbances of the sensor measurement processes, (5b) Jamming of the chamber during its movement
	(6) External disturbances	(6a) Strong currents, (6b) Obstacles below the water surface (leading to thruster blockage, (6c) Obstacles above the water (branches of trees), (6d) Strong wave movements during measurements
Mission evaluation	(7) Errors during data backup and preparation	(7a) Overwriting data, (7b) Errors in data recording, (7c) Loss of storage media, (7d) Loss of data records

654
655

Table 3. MARP-FG robot error monitoring components. ‘Range’ summarizes the maximum distance to the supervisor, limited by visibility or range of wireless communication. ‘Transferred data’ specifies what can be transmitted via individual channels. The detectable ‘error modes’ with the information provided (numeration reference to Table 2).

Item	**Range [m]**	**Transferred data**	**Identifiable error modes (Table 2)**
Position lights	≤ 2500 (nighttime)	Position of the robot and its changes, (particularly during nighttime)	3ab, 4a
Illuminated ring with 24 LEDs	≤ 1000 (nighttime)	Abstract state modes such as “autonomous cruise” or “Measurement in progress”	4ab (knowing the specified time periods)
Telemetry	≤ 500	Status of the robot, its position and related changes, water depth, battery status	1ab, 2ab, 3ab, 6d
Webserver of the chamber system	≤ 20	Current data of the momentary measurement of the chamber	4ab, 5a
Gas samples	0	Implicit data in the form of gas samples taken in parallel with the measurement	5a
Chamber and MARP/FG log files	0	Complete overview of the mission and measurement data of a campaign	3ab, 6d

Fig. 1. An expanded implementation of the MARP-FG concept supports a payload capacity of 100 kg. This enables the platform to carry an ultrasound scanning system or, shown here, a winch with a multisensor probe capable of descending to depths of up to 70 m water depth. The thrusters are Minn Kota electric drives

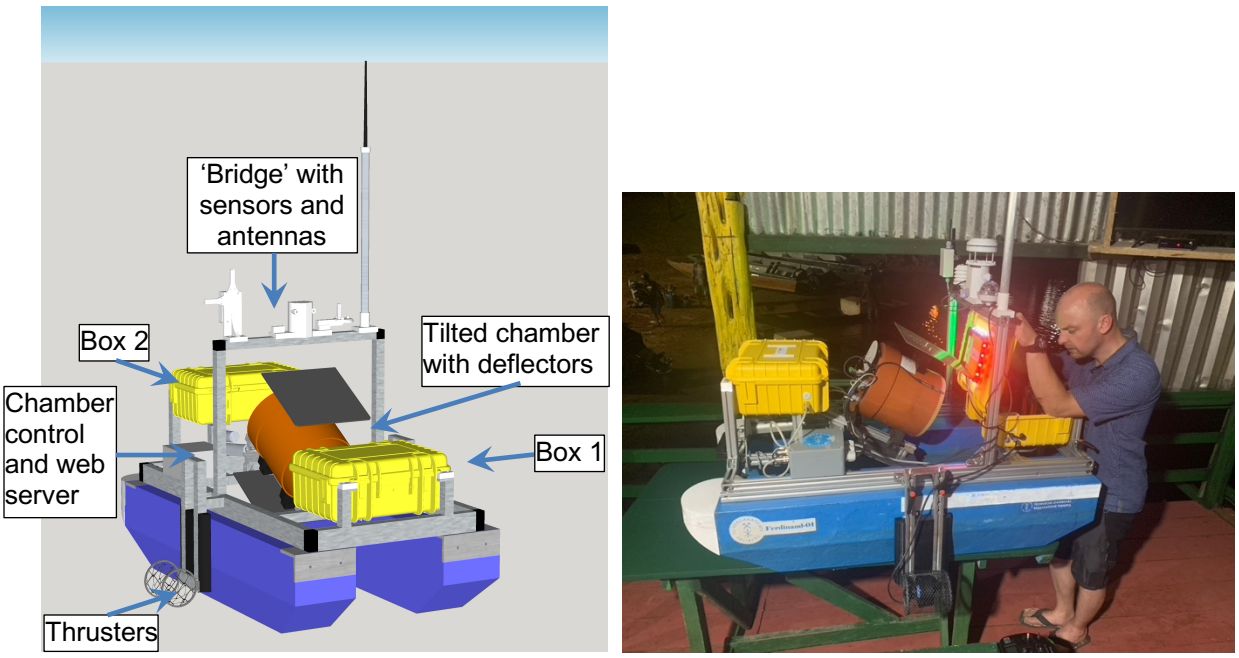

664

665 **Fig. 2. a)** MARP-FG with chamber system. On top, communication antennas, and micrometeorological
666 sensors for wind, humidity temperature and precipitation (white). Below the bridge, at rear, the chamber-tilting
667 mechanism, and the automatic gas sampling box 2 (yellow). Two thrusters are mounted at the center. The
668 chamber (open during transport and flushing) sits in the center inside (orange); deflector shields are visible
669 (gray). In the front: Power supply and positioning equipment in box 1 (yellow). **b)** The real MARP-FG prior to a
670 launch. See text for more detail

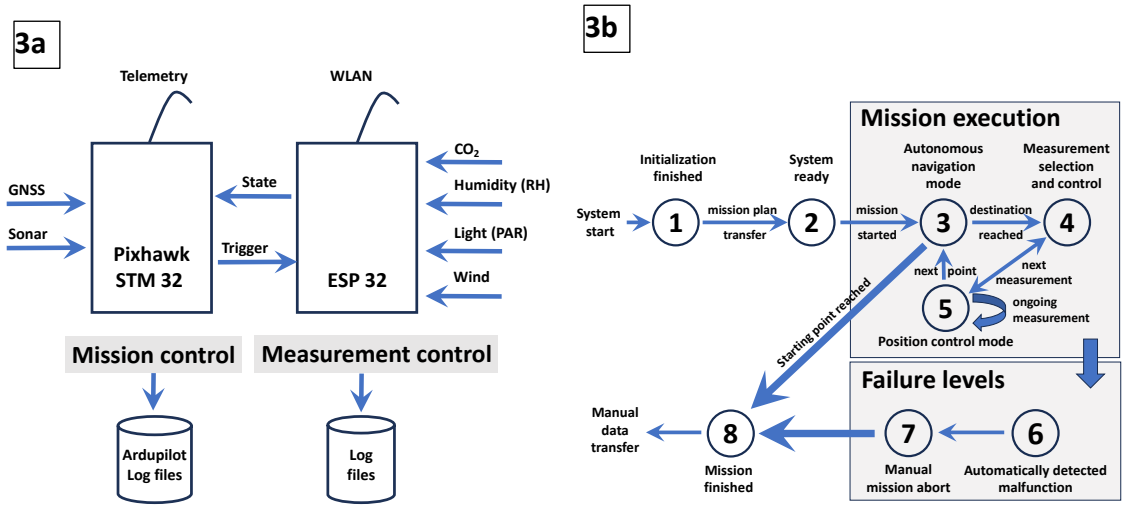

Fig. 3a. Robotic platform architecture. L: Components required for autonomous navigation (Mission control). R: Integration of the actual mission sensors (Measurement control). **Fig. 3b.** Mission steps as state machine. The implementation of a measurement task is sequenced in eight states (1–8) that can be divided into three levels: initialization, mission execution and failure. States 3–5 are central. Here, the robot realizes the actual measurement task and navigates between positions or executes changing programs at individual positions

671

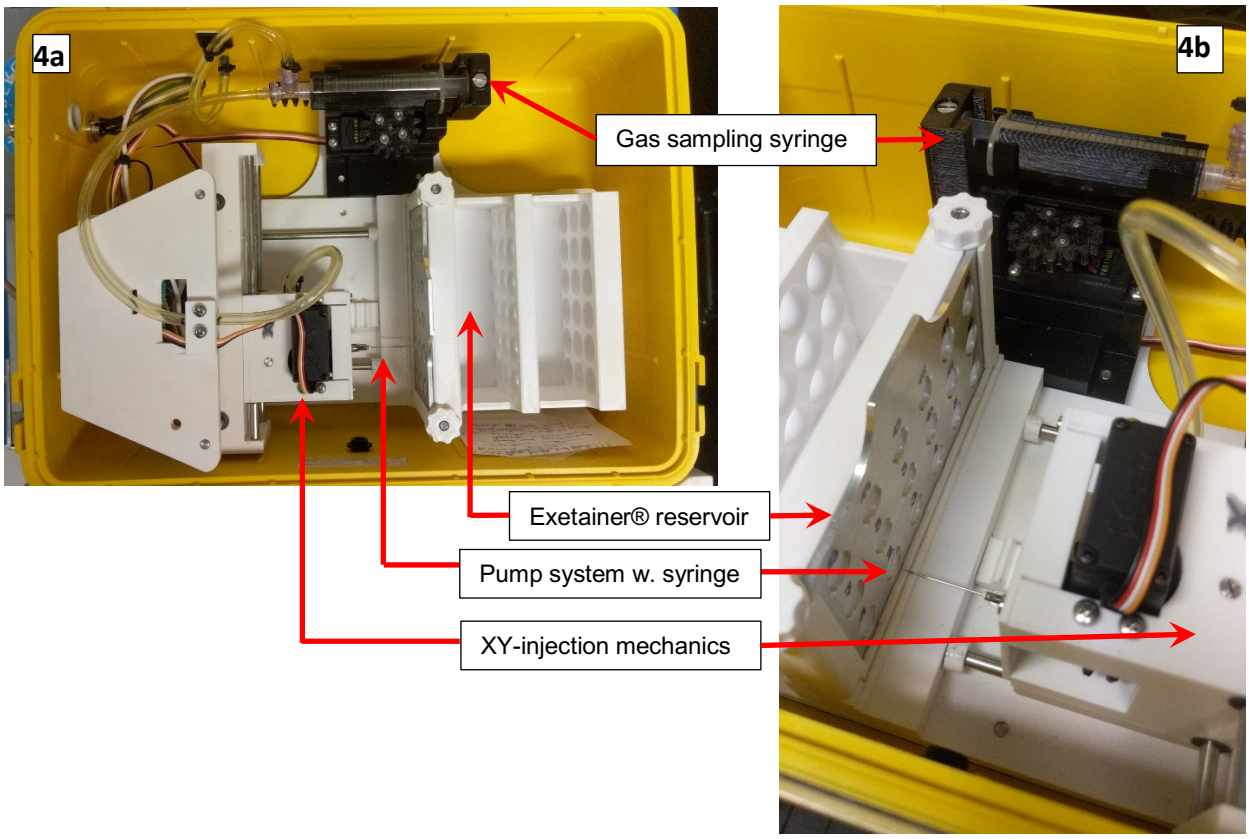

672 **Fig. 4.** Overview of the gas sampling unit (a) and details (b). **a)** The three central components: Pump system
673 (10 mL) in the upper part, the autonomously operating injection mechanism and the reservoir for 3x6
674 Exetainers® on the right. **b)** The injection needle (at front) through which gas is being filled into the evacuated
675 Exetainers® (left).

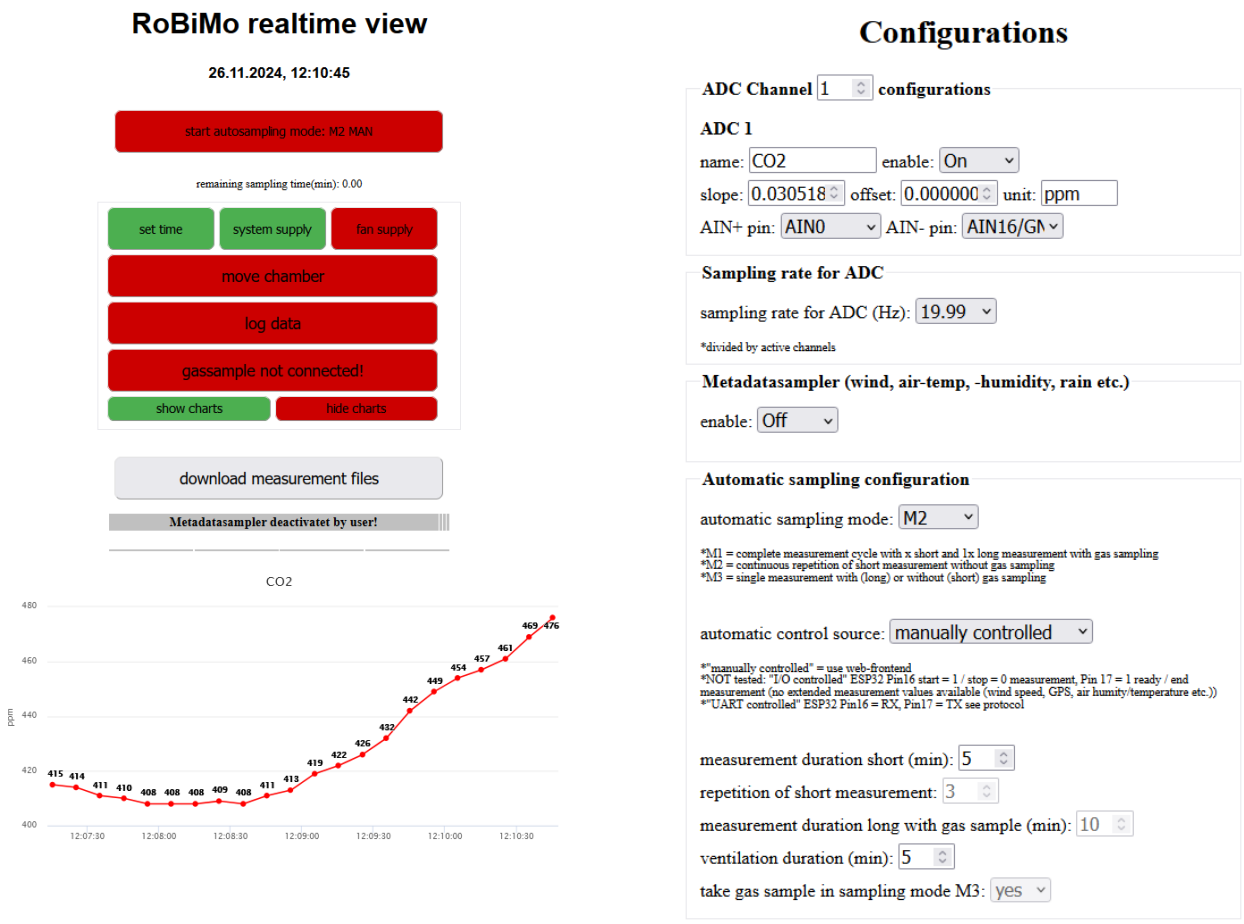

Fig. 5. Exemplary screenshots of the Website provided by the measurement system web server. It controls configuration parameters and visualizes the ongoing data aggregation in a diagram.

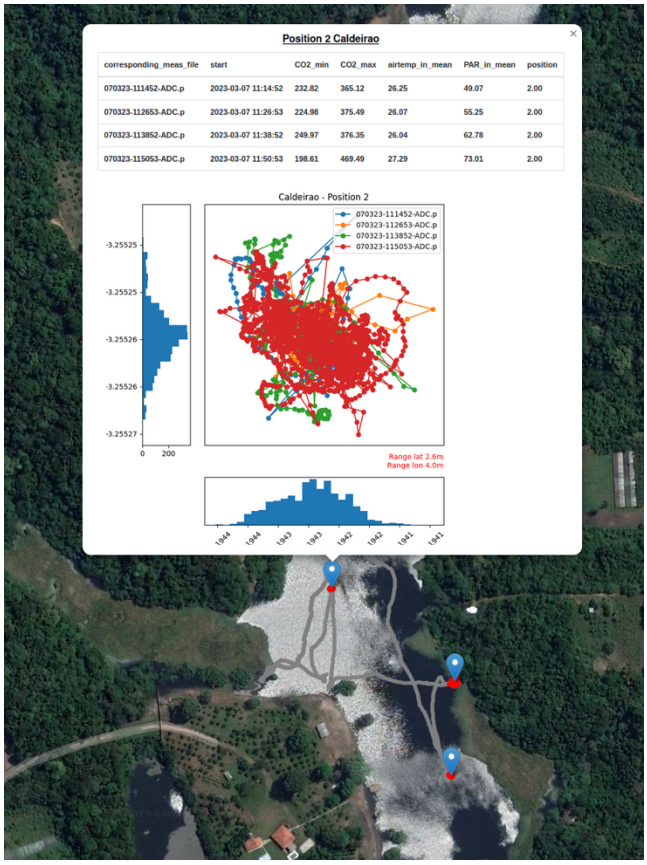

Fig. 6. MARP-FG tracks (grey) between sampling positions on Lake Caldeirão, Amazonas, Brazil. The inset shows the platform movement at a specific position while performing measurements (4th RoBiMo/Trop campaign with minor flaws in autonomous-cruising capability). During measurements the position of the system varies in an area of 4 x 2.6 m. The histograms for latitude and longitude illustrate that the maximum deviation is caused by outliers

Fig. 7. Platform development from September 2021 to March 2023. Subsequent progress until August 2023 is invisible (= software improvements)